

# Quantifying the role of wood density in explaining interspecific variation in growth of tropical trees

Emily J. Francis<sup>1</sup>  | Helene C. Muller-Landau<sup>2</sup> | S. Joseph Wright<sup>2</sup> |  
Marco D. Visser<sup>3</sup> | Yoshiko Iida<sup>4</sup> | Christine Fletcher<sup>5</sup> | Stephen P. Hubbell<sup>6</sup> |  
Abd. Rahman Kassim<sup>5</sup>

<sup>1</sup>Department of Earth System Science,  
Stanford University, Stanford, California

<sup>2</sup>Smithsonian Tropical Research Institute,  
Apartado Postal 0843-03092, Panamá,  
República de Panamá

<sup>3</sup>Department of Ecology and Evolutionary  
Biology, Princeton University, Princeton,  
New Jersey

<sup>4</sup>Kyushu Research Center, Forestry and  
Forest Products Research Institute,  
Kumamoto, Japan

<sup>5</sup>Forestry and Environment Division, Forest  
Research Institute Malaysia, Kuala Lumpur,  
Malaysia

<sup>6</sup>Ecology and Evolutionary Biology,  
University of California, Los Angeles,  
California

## Correspondence

Emily J. Francis, Department of Earth  
System Science, Stanford University,  
Stanford, CA, 94305-4216, U.S.A.  
Email: efrancis@stanford.edu

## Funding information

U.S. National Science Foundation

Editor: Andrew Kerkhoff

## Abstract

**Aim:** To evaluate how wood density relates to tree growth rates in simple models and two tropical forests.

**Location:** Barro Colorado Island, Panama; and Pasoh Forest Reserve, Malaysia.

**Time Period:** 1986–2010.

**Major Taxa Studied:** Trees.

**Methods:** We derived expected relationships of wood density with diameter growth at a given diameter under a null hypothesis that aboveground biomass growth is independent of wood density, and an alternative hypothesis that biomass growth scales with crown area, which itself increases with wood density. We tested these assumptions and predictions through analyses of interspecific relationships of wood density with height, crown area and diameter growth at constant diameter in two tropical forests.

**Results:** Height was unrelated to wood density, whereas crown areas showed a slightly positive relationship to wood density. Thus, the expected exponent of diameter growth with wood density was equal to minus one under the null hypothesis, and equal to the exponent of crown area with wood density minus one under the alternative hypothesis. Empirical relationships of diameter growth and biomass growth with wood density were broadly consistent with the null hypothesis that biomass growth is unrelated to wood density at both sites, except in trees < 13 cm in diameter at Barro Colorado Island, which showed more negative relationships.

**Main conclusions:** Although most previous analyses of growth with wood density have examined linear relationships, simple models suggest that both tree diameter growth and tree biomass growth are power functions of wood density. Analyses in two tropical forests showed that aboveground biomass growth was approximately constant with wood density, and thus, that diameter growth was inversely proportional to wood density, for most tree sizes, although confidence intervals on the scaling exponents were broad. More negative relationships of growth with wood density at small sizes might reflect differential environmental filtering, in which higher wood density trees are found in less favourable understorey environments.

## KEYWORDS

aboveground biomass, allometry, Barro Colorado Island, forest carbon, forest demography, functional trait, Pasoh, tree growth, wood density

## 1 | INTRODUCTION

Functional traits are attributes of organisms that are associated with their life-history strategies and therefore have the potential to predict their demographic performance (Reich et al., 2003; Westoby & Wright, 2006). In tropical forests, the functional trait that is most strongly and consistently associated with the growth and survival of tree species is wood density. Globally, wood density varies by more than an order of magnitude, from 0.11 to 1.39 g/cm<sup>3</sup> (Chave et al. 2006). Denser wood is associated with slower diameter growth rates, higher survival rates and higher shade tolerance among tropical trees (King, Davies, Supardi, & Tan, 2005; Kraft, Metz, Condit, & Chave, 2010; Muller-Landau et al., 2006; Philipson et al., 2014), and these relationships have been embedded in ecosystem models; for example, Moorcroft, Hurtt, and Pacala (2001).

Multiple studies have reported a negative relationship between diameter growth and wood density in tropical trees (Hérault et al., 2011; Iida, Kohyama et al., 2014; Iida, Poorter et al., 2014; King, Davies, Tan, & Noor, 2006; King et al., 2005; Nascimento et al., 2005; Philipson et al., 2014; Poorter et al., 2008, 2010; Rüger, Wirth, Wright, & Condit, 2012; Wright et al., 2010). This negative relationship can be explained by the fact that a species with high wood density by definition invests more biomass into each unit of diameter growth (Chave et al., 2009). Wood density may have other influences on tree growth rate in addition to this purely dimensional effect, but previous analyses focusing on diameter growth cannot separate the higher biomass cost of denser wood from other possible effects of wood density on tree growth (Wright et al., 2010). Furthermore, most prior studies, except King et al. (2006), have analysed linear relationships between tree diameter growth rates and wood density (Hérault et al., 2011; Iida, Kohyama et al., 2014; Iida, Poorter et al., 2014; King et al., 2005, 2006; Nascimento et al., 2005; Philipson et al., 2014; Poorter et al., 2008, 2010; Rüger et al., 2012; Wright et al., 2010). However, we show below that the influence of wood density on diameter growth is multiplicative, thus analyses with respect to log-transformed wood density are more informative than analyses with respect to untransformed wood density.

In addition to the straightforward effect of wood density on diameter growth at a given diameter, there is evidence to suggest that wood density could also affect tree biomass growth rate at a given diameter. Higher wood density may enable greater tree height, crown area and/or crown depth at a given trunk diameter, thus positively influencing whole-plant carbon gain (Aiba & Nakashizuka, 2009; Bohlman & O'Brien, 2006; Iida et al., 2012). Higher wood density may also be associated with reduced maintenance and respiratory costs, as a result of enhanced resistance to branch breakage and greater xylem resistance to embolism (Anten & Schieving, 2010; Hacke, Sperry, Pockman, Davis, & McCulloh, 2001), thereby increasing the carbon available for growth. In contrast, high wood density is associated with lower vessel area (Hietz, Rosner, Hietz-Siefert, & Wright, 2017), which may lead to lower light-use efficiency and photosynthetic capacity (Chave et al., 2009). Interspecific relationships with wood density may also reflect environmental filtering, as species with high wood density are more likely to be found in

darker environments (Wright et al., 2010) and on soils with lower fertility (Muller-Landau, 2004; Quesada et al., 2012), which would influence observed species-average carbon gain and growth.

We argue that to gain a better understanding of how wood density influences tree growth rates, observed relationships should be compared quantitatively with specific predictions from alternative models. We first derive such predictions for two models; a null hypothesis, under which aboveground biomass growth is independent of wood density, and an alternative hypothesis, under which it is proportional to crown area, itself assumed to be a power function of wood density. In both cases, we make simplifying assumptions regarding how height and biomass allometries relate to wood density. We then analyse empirical data on allometries and growth rates for hundreds of tropical tree species at two sites to test and parameterize the underlying assumptions regarding how wood density relates to allometry, and to quantitatively test the resulting predictions regarding the relationship of wood density to growth.

## 2 | THEORY

### 2.1 | Null hypothesis: Aboveground biomass growth at a given diameter is unrelated to wood density

We first derive the expected relationship of growth rate to wood density under a null hypothesis, in which aboveground biomass growth at a given trunk diameter is unrelated to wood density. This is the relationship (or lack thereof) that we would expect if interspecific variation in wood density had no relationship with interspecific variation in height or crown area allometries, expected light environment at a given diameter, light-use efficiency, whole-plant respiratory costs or proportional allocation of carbon to woody growth, and influences diameter growth purely through its influence on the carbon content of a given diameter increment.

Denoting trunk diameter with  $D$  and aboveground biomass with  $M$ , we can express our central assumption in the equation:

$$\frac{dM}{dt} = g(D)$$

that is, biomass growth depends only on diameter, expressed as a general function  $g(D)$ , and not at all on wood density, denoted  $\rho$ .

For simplicity, we further assume an approximate generic tree biomass allometry equation, in which aboveground biomass ( $M$ ) is linearly related to the product of wood density ( $\rho$ ), basal area and tree height ( $H$ ), with the slope  $c$  of the pantropical biomass allometry equation from Chave et al. (2014), as follows:

$$M(D) = c\rho D^2 H(D)$$

Finally, we assume that height is a piecewise power function of diameter (that is, the log of height is a piecewise linear function of the log of diameter) so that for diameters  $D$  near  $\bar{D}$  we can write:

$$H(D) = \bar{a} \bar{D}^{\bar{b}}$$

where  $\bar{a}$  and  $\bar{b}$  are the coefficients of the power function for diameters near  $\bar{D}$ . Note that the independence of height with respect to wood density means specifically that the log-log slope of height at a given

diameter versus wood density is zero; this is the assumption we test in our empirical analyses.

Then it follows that diameter growth  $\frac{dD}{dt}$  at a given diameter  $D=\bar{D}$  has the following log–log relationship with wood density (details in Supporting Information Appendix S1):

$$\log\left(\frac{dD}{dt}\Big|_{D=\bar{D}}\right) \approx \log\left(\frac{g(\bar{D})}{c(\bar{b}+2)\bar{D}H(\bar{D})}\right) - \log \rho$$

Thus, the expected slope of the relationship between the logarithm of diameter growth rate at a given diameter and the logarithm of wood density is equal to negative one.

## 2.2 | Alternative hypothesis: Aboveground biomass growth is proportional to crown area, which is a power function of wood density

Alternatively, we could assume that whole-tree biomass growth rate is proportional to crown area, an assumption consistent with the idea that potential carbon gain increases with light capture (King et al., 2005; Wyckoff & Clark, 2005). Denoting crown area with  $C$ , we express this as follows:

$$\frac{dM}{dt} = kC(D)$$

Where  $k$  is a constant relating crown area to biomass growth. Let us assume further that crown area at a given diameter is itself a power function of wood density, consistent with the empirical analyses to be presented here:

$$C(D) = \rho^r f(D)$$

We retain the previous assumptions regarding biomass and height allometries.

In this case, biomass growth rates at a given diameter  $D=\bar{D}$  will be related to wood density as follows:

$$\log\left(\frac{dM}{dt}\Big|_{D=\bar{D}}\right) \approx \log(kf(\bar{D})) + r \log \rho$$

and diameter growth rates at a given diameter will be related to wood density as follows:

$$\log\left(\frac{dD}{dt}\Big|_{D=\bar{D}}\right) \approx \log\left(\frac{kf(\bar{D})}{c(\bar{b}+2)\bar{D}H(\bar{D})}\right) + (r-1) \log \rho$$

Thus, the log–log slope of diameter growth at a given diameter with wood density is expected to be exactly equal to the log–log slope of crown area with wood density minus one.

## 3 | MATERIALS AND METHODS

### 3.1 | Study sites and species

Data were collected in or near two 50-ha forest dynamics plots in the Center for Tropical Forest Science plot network, on Barro Colorado Island (BCI) in central Panama, and in the Pasoh Forest Reserve in Malaysia. The

forest on BCI (9°9' N, –79°51' W) is a moist tropical rain forest, with mean annual rainfall of 2,551 mm and a dry season that lasts from December to April. Most of the plot is located on a level plateau at 140 m a.s.l. atop andesitic oxisol soils. There are 304 tree and shrub species in the plot (Condit, 1998). The Pasoh plot (2°59' N, 102°18' E) hosts a lowland dipterocarp rain forest on a level alluvial plain at c. 100 m a.s.l. Rainfall is aseasonal, averaging 1,810 mm annually, and there is typically one 20-day period without rain during each year. There are c. 840 tree and shrub species in the plot (Manokaran et al., 2004).

We restricted our analyses to non-palm species that can obtain canopy size, as evidenced by a maximal diameter in our datasets of > 35 cm. We excluded palms because they do not generally grow in diameter. We excluded shorter-statured species because we aimed to investigate how patterns change with diameter between 2 and 35 cm and wanted to isolate the pure effects of diameter without confounding effects of short-statured species dropping out of the analyses at larger size classes.

### 3.2 | Wood density data

Wood density varies within species and within trees, but intraspecific variation is less than interspecific variation (Hietz, Valencia, & Wright, 2013). For this analysis, we used species-average wood density values. Species-average wood density values were from on-site measurements for all BCI species and 16 out of 130 Pasoh species (Wright et al., 2010). Tree cores were taken from within 15 km of BCI and from the once-logged (1970s) portions of the Pasoh Forest Reserve. Each core was broken into pieces < 5 cm long, on average four pieces per core. The fresh volume of each core was measured by water displacement, and oven-dry mass was measured after drying at 100 °C for samples from BCI and 60 °C for samples from Pasoh. The wood density (technically wood specific gravity) of each tree was calculated as the average of the dry mass divided by the fresh volume of each piece of wood, weighted by the area of the annulus from which each wood piece originated. Species-specific values were calculated as averages over four to seven trees per species. For all other species from Pasoh, wood density was based on Southeast Asian regional averages of values from the global wood density database (Chave et al., 2006; Zanne et al., 2009).

### 3.3 | Allometric analyses

We fitted species-specific allometric models relating crown area and height to trunk diameter at both sites. For BCI, we used a compilation of seven datasets, one of which was collected on Gigante peninsula on the mainland adjacent to BCI in the Barro Colorado National Monument (Supporting Information Appendix S2, Table S1). Allometry data from Pasoh were collected by Iida et al. (2012) and Visser (unpublished observations, Visser 2005). All diameter measurements were made at 1.30 m height, or above buttresses. Trees with damaged crowns were deliberately avoided for all measurements on BCI. Thus, we excluded trees with damaged crowns (as recorded by Y. Iida) from the Pasoh dataset (c. 10% of trees in the original dataset).

Prior studies have suggested that crown area and height allometries are power functions for some diameter ranges, but not all (Muller-

Landau et al., 2006). We chose to model crown area and height allometries with generalized additive models, hereby referred to as GAMs, because they require no prior assumptions about the functional form of the relationship, and allow for variability in functional forms among species (e.g., Visser et al., 2016). We then used the species-specific models to predict the expected crown diameters and the heights of a tree at each integer diameter from 2 to 35 cm (hereafter referred to as reference diameters). To analyse how interspecific variation in crown area and height at a given diameter relate to wood density, we regressed the  $\log_{10}$ -transformed predicted crown diameters and predicted heights against  $\log_{10}$ -transformed wood density for each reference diameter. We excluded species with a minimal diameter  $> 2$  cm, a maximal diameter  $< 35$  cm, and species that did not have data within 15 cm of the maximal diameter for prediction (species with data  $> 50$  cm but not between 35 and 50 cm). We did this in order to ensure that the predicted crown area or height was not outside of the range of the observed crown area or height and to ensure that the calculated slopes would not change significantly with diameter as a result of species 'dropping out' of the regression because their ranges differed. Application of these restrictions left 34 species from BCI and 34 species from Pasoh for the diameter-crown area analysis, and 59 species from BCI and 24 species from Pasoh for the diameter-height analysis. To characterize between-site differences in average allometries, we also conducted the same analyses for the pooled data for all species at each site combined (Supporting Information Appendix S2, Figure S1).

### 3.4 | Growth analyses

The 50-ha forest census plots on BCI and in Pasoh were established in 1980 and 1986, respectively, and have been re-censused at 5-year intervals. The censuses encompass all individuals of free-standing woody plants (no lianas) with a trunk diameter at 1.3 m height or above buttresses  $\geq 1$  cm. All individual stems on each plot are tagged, mapped, identified to species and measured in diameter when they first enter the census; at subsequent censuses, they are recorded as alive or dead, and their diameter is measured if alive. Each census interval at each plot thus provides growth and survival data for  $> 200,000$  individual trees of hundreds of species. We excluded the first two census intervals from BCI (1980–1990) because of methodological differences in how diameter was measured in small and large trees (Condit, 1998).

To analyse how size-specific diameter growth varies in relation to wood density, we first fitted the relationships of growth with initial diameter within species. We excluded from analysis trees with multiple or broken stems, records with an initial diameter  $> 50$  cm, records in which the height of the measurement changed between census intervals, and records that showed unrealistic growth rates (any tree with a diameter measurement  $> 4$  SD below its previous diameter measurement or any tree showing a diameter growth rate  $> 75$  mm/year; Condit et al., 2006). For each species, we modelled absolute diameter growth rate (in square centimetres per year) as a function of initial

diameter using a GAM with normal errors, following Visser et al. (2016).

We then used the fitted species-specific growth functions to calculate the expected diameter growth for each species at every reference diameter. We regressed species' predicted  $\log_{10}$ -transformed absolute diameter growth against  $\log_{10}$ -transformed wood density at each reference diameter. We analysed each species with  $\geq 25$  individuals, with a minimal diameter  $< 2$  cm, and a maximal diameter  $> 35$  cm. We excluded four BCI species and three Pasoh species for which the GAMs predicted negative growth rates at some diameters between 2 and 35 cm. This left 106 BCI species and 130 Pasoh species for analysis of diameter growth with wood density.

We then used the modelled relationships of growth and height with diameter together with a generalized biomass allometry equation to estimate biomass growth at each reference diameter for every species for which both growth and height relationships were available. Specifically, for each reference diameter  $D$ , we calculated the following:

$$\frac{dM}{dt} = c\rho D \left( D \frac{dH}{dD} + 2H(D) \right) \frac{dD}{dt}$$

where  $c$  is the coefficient of the pantropical biomass allometry model from (Chave et al., 2014),  $\rho$  is species-specific for wood density, the derivative of the height function and the height at a reference diameter were based on the species-specific GAMs fitted to the height data, and the diameter growth at the reference diameter was based on the species-specific GAMs fitted to the growth data. We then regressed the logarithm of estimated biomass growth against the logarithm of wood density for each site and reference diameter. We used only species included in the height-diameter allometry analysis and the diameter growth - wood density analysis, leaving 48 BCI species and 24 Pasoh species for analysis of biomass growth with wood density. R Code for analyses is provided in Supporting Information Appendix S3.

## 4 | RESULTS

### 4.1 | Allometry

Tree height at a given diameter was not significantly associated with wood density at BCI or in Pasoh, except for trees at 2 cm diameter at BCI, and the estimated log-log slopes of height with wood density were near zero for all diameters, with narrow confidence intervals (Figure 1). Crown area at a given diameter showed a significant positive correlation with wood density at BCI and Pasoh at some diameter values but not others (Figure 2). Crown area showed a slight positive correlation with wood density for trees 9–35 cm diameter at BCI and trees 3–18 cm diameter at Pasoh (Figure 2). The estimated log-log slopes of crown area with wood density were between 0 and 1 at all sizes at both sites, with site-specific patterns of variation with diameter, and wide confidence intervals that encompassed zero for small trees at BCI and large trees at Pasoh (Figure 2).

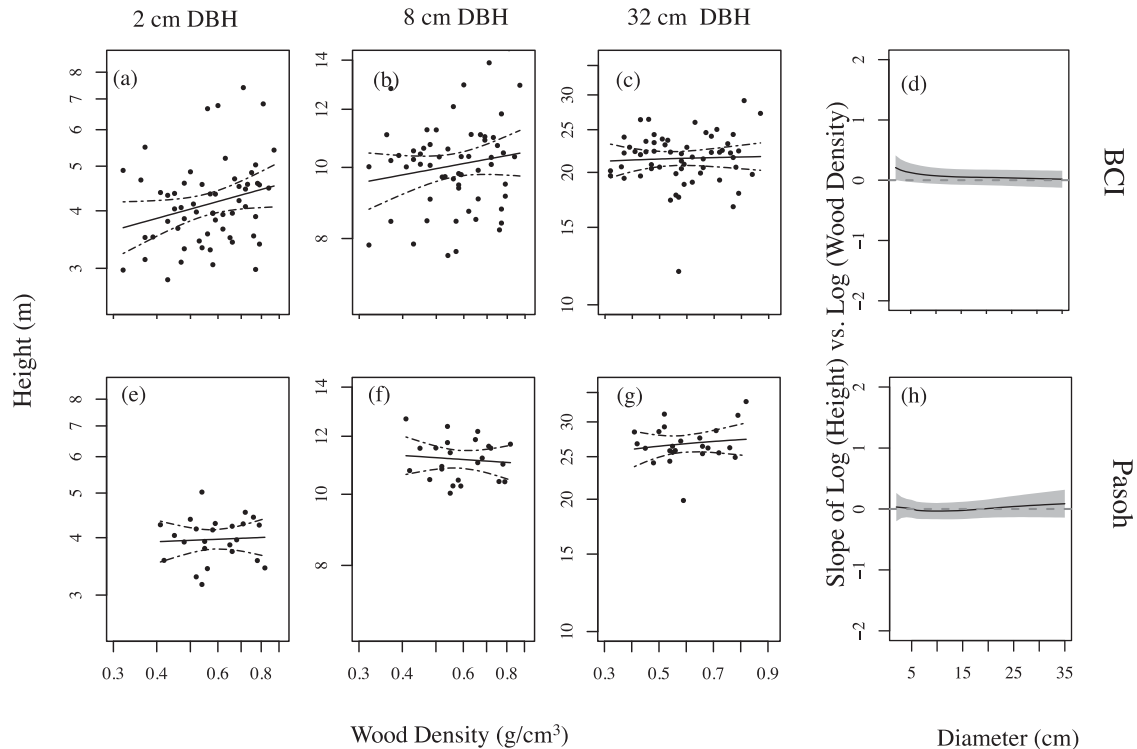


**FIGURE 1** Relationships of species-specific wood density versus tree height at a given trunk diameter vary with reference diameter and between Barro Colorado Island (BCI, top row, a-d) and Pasoh (bottom row, e-h). Scatterplots show the relationships for reference diameters of 2 cm (a, e), 8 cm (b, f) and 32 cm (c, g) with regression lines shown as solid lines and their confidence intervals as dashed lines. The slopes of the regression of  $\log(\text{height})$  against  $\log(\text{wood density})$  are plotted as black lines against reference diameter within each site (d, h). Slopes of relationships of  $\log(\text{height})$  versus  $\log(\text{wood density})$  are not significantly different from zero at all reference diameters greater than 2 cm (95% confidence intervals are shaded in grey behind the lines).

## 4.2 | Growth

$\log_{10}$ -transformed diameter growth was negatively related to  $\log_{10}$ -transformed wood density at all sizes at both sites (Figure 3). Slopes of relationships between  $\log_{10}$ -transformed diameter growth and  $\log_{10}$ -transformed wood density were significantly more negative than the value ( $-1$ ) predicted by the null hypothesis that biomass growth is invariant with wood density for trees 2–13 cm in diameter at BCI, and were not significantly different from the value predicted by the null hypothesis at all other diameters at both sites (compare continuous black line and shaded confidence intervals with grey dashed line in Figure 3d,h). The expected slopes based on the alternative hypothesis differed between BCI and Pasoh, reflecting their differing crown area relationships (compare the black dashed lines between Figure 3d,h, which parallel Figure 2d,h). At BCI, slopes were consistently more negative than predicted based on the alternative hypothesis that biomass growth scales with crown area, whereas at Pasoh the slopes trended lower but were significantly more negative only for trees 4–20 cm in diameter (compare continuous black line and shaded confidence intervals with black dashed line in Figure 3d,h).

$\log_{10}$ -transformed biomass growth was not significantly related to wood density at any diameter at either site, consistent with the null hypothesis (Figure 4). Confidence intervals were large and encompassed both the slopes predicted from the null hypothesis (compare

grey dashed line with shaded confidence intervals in Figure 4) and the slopes predicted from the alternative hypothesis (compare black dashed line with shaded confidence intervals in Figure 4). The small differences in patterns relative to the null hypothesis between the diameter growth and biomass growth relationships are mostly attributable to the smaller set of species included in the biomass analysis, which required height allometry data. When diameter growth analyses were run for the same set of species, results paralleled those for biomass growth (Supporting Information Appendix S2, Figure S2).

## 5 | DISCUSSION

Here, we presented a theoretical framework for quantitative evaluation of the relationship of diameter growth to wood density in light of specific hypotheses and applied it to empirical data from two tropical forests. By comparing the expected with the empirical relationships, we found that negative relationships between diameter growth and wood density were consistent with the hypothesis that biomass growth is invariant with wood density for all tree sizes at Pasoh and for larger trees at BCI, but suggest that biomass growth decreases with wood density in trees  $< 13$  cm in diameter at BCI. Higher wood density was associated with larger crown areas at both sites, which led to the expectation that biomass growth would increase with wood density under

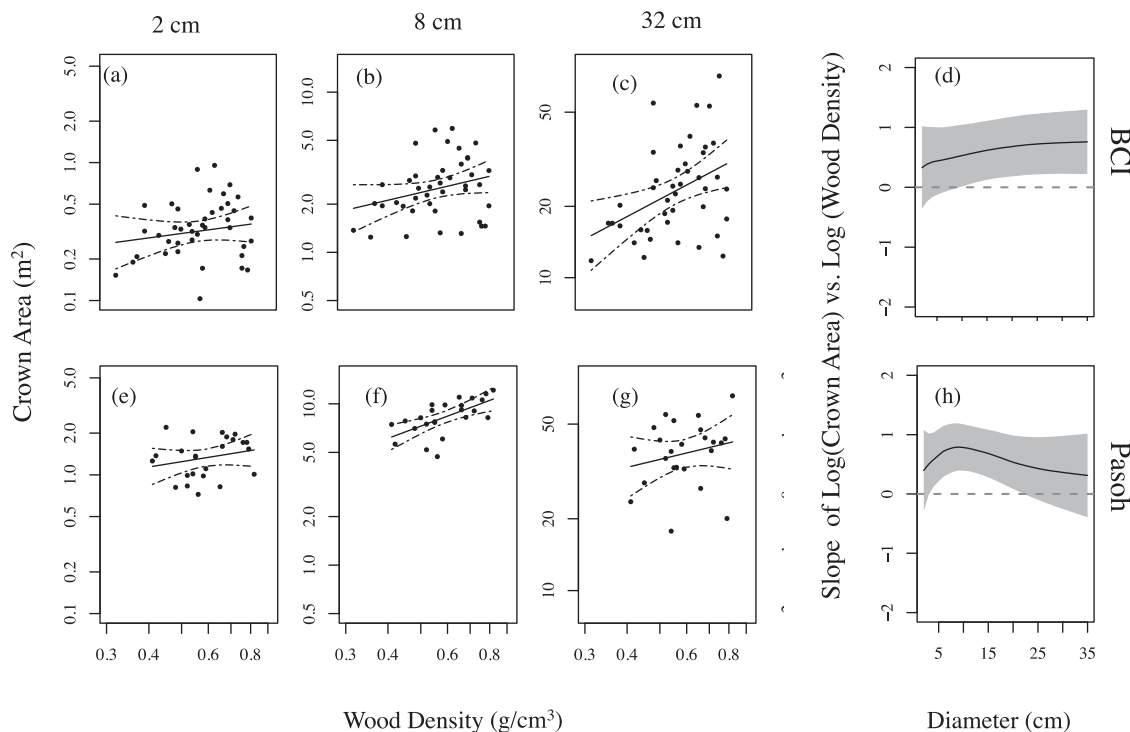


**FIGURE 2** Relationships of species-specific wood density versus crown area at a given trunk diameter vary with reference diameter and between Barro Colorado Island (BCI, top) and Pasoh (bottom). Scatterplots show the relationships for reference diameters of 2 cm (a, e), 8 cm (b, f) and 32 cm (c, g), with regression lines shown as solid lines and their confidence intervals as dashed lines. The slopes of the regression between log(crown area) and log(wood density) are plotted against reference diameter within each site (d, h). Slopes of relationships of log(crown area) versus log(wood density) are significantly greater than zero at some reference diameters but not others (95% confidence intervals are shaded in gray behind the lines).

the alternative hypothesis that biomass growth is proportional to crown area, but this hypothesis was not supported by observed patterns. This work builds on numerous previous studies finding that wood density is negatively related to diameter growth (Héroult et al., 2011; Iida, Kohyama et al., 2014; Iida, Poorter et al., 2014; King et al., 2005, 2006; Nascimento et al., 2005; Philipson et al., 2014; Poorter et al., 2008, 2010; Rüger et al., 2012; Visser et al., 2016; Wright et al., 2010).

To predict a set of null and alternative expectations about the relationship between wood density and diameter growth, we assumed that wood density showed no relationship with height at a given diameter. Consistent with this assumption, we found that height at a constant diameter was unrelated to wood density, except for trees at 2 cm diameter on BCI (Figure 1). This agrees with previous findings (Aiba & Nakashizuka, 2009; King et al., 2006) and theoretical work suggesting that dense wood confers no mechanical advantage for increased height at a given diameter (Anten & Schieving, 2010). Despite using a similar dataset, our results differed slightly from what would be expected from Iida et al. (2012), who found that wood density was negatively related to diameter at a given height. However, we excluded small-statured trees (trees with a maximal diameter < 35 cm) from our analyses. Large-statured trees are taller at a given diameter than small-statured trees (Bohman & O'Brien, 2006). Thus, our dataset probably showed a smaller total range in height than that of Iida et al. (2012), which might explain the differences.

In agreement with previous studies, we found that wood density showed a significant positive relationship to crown area at a given

diameter, with statistically significant relationships at many (but not all) sizes (Figure 2d,h). Prior studies have reported larger crown areas for trees with high wood density (Iida et al., 2012) and for shade-tolerant trees (Bohman & O'Brien, 2006; Sterck, Van Gelder, & Poorter, 2006), which also have higher wood densities (Augsburger & Kelly, 1984). Dense wood is more flexible (Anten & Schieving, 2010), which might enhance branch resistance to breakage. We hypothesized that the larger crown areas of species with high wood density would increase whole-plant light capture and therefore have a positive effect on their growth rates (Iida, Poorter et al., 2014; King et al., 2005; Wyckoff & Clark, 2005). Based on the assumption that aboveground biomass growth is proportional to crown area, we predicted that the slope of the relationship between log<sub>10</sub>-transformed diameter growth and log<sub>10</sub>-transformed wood density would be one less than the slope of the relationship between crown area and wood density at the same diameter (Supporting Information Appendix S1).

## 5.1 | Effects of wood density on tree growth

Empirical relationships of log<sub>10</sub>-transformed growth with log<sub>10</sub>-transformed wood density were consistent with the null hypothesis of no relationship between aboveground biomass growth and wood density, except in small trees at BCI, which showed slower diameter growth rates than expected under the null hypothesis (Figure 3d,h). To explore the possibility that the larger crown areas of species with high wood density are advantageous for biomass growth, we also tested an

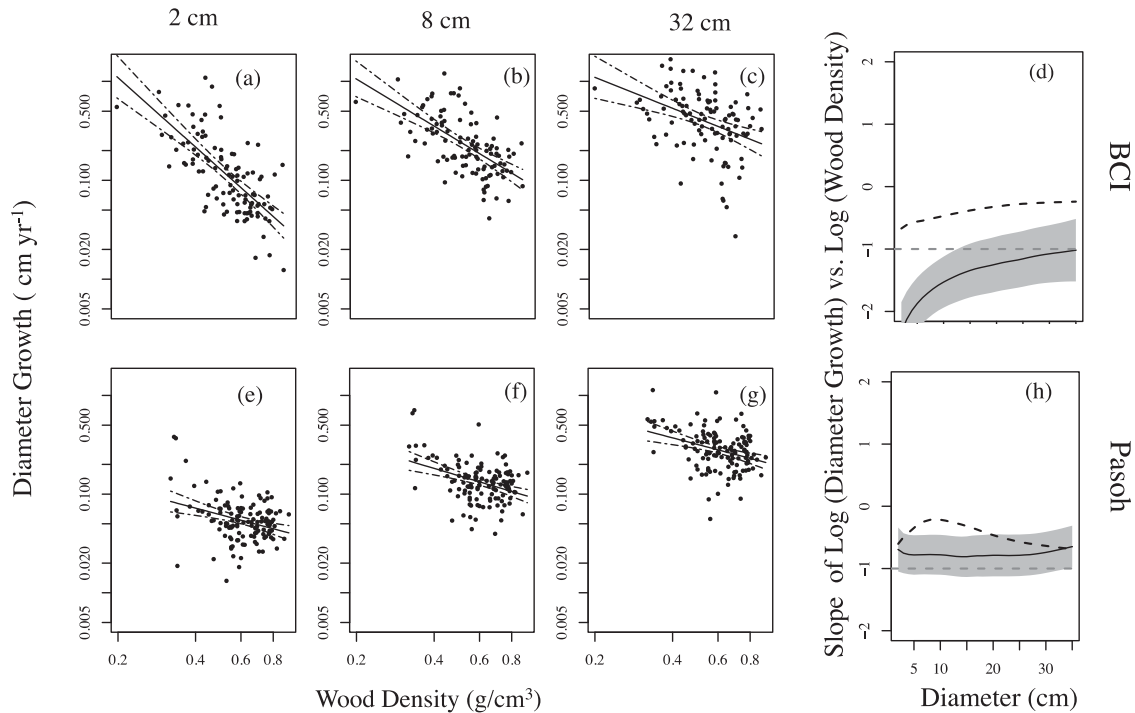


**FIGURE 3** Relationships of species-specific diameter growth rate versus wood density vary with reference diameter and between BCI (a-d) and Pasoh (e-h). Scatterplots show relationships at 2 cm diameter (a, e), 8 cm diameter (b, d), and 32 cm diameter (c, g). The slopes of the relationships between log(diameter growth rate) and log(wood density) are plotted against diameter (d, h), where the black line shows the empirical slopes, the dashed gray line shows the slope predicted from the null hypothesis that biomass growth is constant with wood density, and the dashed black line shows the slopes predicted from the alternative hypothesis that biomass growth scales with crown area. The slopes are not significantly different from slopes predicted from the null hypothesis, except trees smaller than 13 cm at BCI show slopes that are significantly more negative than the null hypothesis (95% confidence intervals are shaded in gray behind the lines).

alternative hypothesis that aboveground biomass growth scales with crown area and is thereby related to wood density. Despite their larger crown areas, species with high wood density did not show significantly faster biomass growth rates.

There are multiple pathways through which wood density could negatively affect tree biomass growth, including not only physiological correlates but also environmental filtering. High wood density is associated with lower xylem vessel area (Hietz et al., 2017), which could limit light-use efficiency and photosynthesis (Chave et al., 2009), and thereby negatively affect tree growth. Species with high wood density are more likely to be found in low-light environments (Augspurger & Kelly, 1984; Poorter et al., 2010), at low soil fertility (Muller-Landau et al., 2006; Quesada et al., 2012) and infested with lianas (Schnitzer & Carson, 2010; Visser, 2016). Environmental filtering with respect to light environment may be especially important for small individuals, which experience highly variable and temporally autocorrelated light environments (Yoda, 1974). At small sizes, species with high wood density at BCI showed significantly slower diameter growth rates than expected under the null hypothesis of constant biomass growth with wood density (Figure 3), although they did not show significantly slower biomass growth than expected under the null hypothesis (Figure 4). This discrepancy occurred because the biomass growth analysis required species-specific height allometry data and thus included far fewer species at BCI (106 species in the diameter growth analysis versus 48 species in the biomass analysis).

There are also potential positive effects of wood density on tree biomass growth. First, there is evidence that species with high wood density have deeper crowns, which could further increase light capture (Augspurger & Kelly, 1984; Bohlman & O'Brien, 2006; Iida et al., 2012). Beyond systematic differences in allometry, high wood density could be advantageous for biomass growth because of reduced maintenance costs, which would increase the carbon available for wood growth. Specifically, high wood density is associated with improved xylem resistance against embolism (Hacke et al., 2001) and branch flexibility (Anten & Schieving, 2010), which may result in less carbon allocated to xylem repair and branch turnover, and more carbon allocated to woody growth. However, our results suggest that these positive effects are balanced or outweighed by the aforementioned negative effects of higher wood density on tree biomass growth. A better understanding of the multiple counteracting effects of wood density on biomass growth could be obtained through future experiments that control for growing conditions (light, soil fertility or liana load), or comparative analyses that account for their differences, for example through independent data on light availability (Lichstein et al., 2010; R uger et al., 2012).

## 5.2 | Metrics in plant functional ecology

We know of one prior study that explored how mass growth relates to wood density. R uger et al. (2012) found that growth in cross-sectional mass (the product of wood density and basal area) was similar in a low

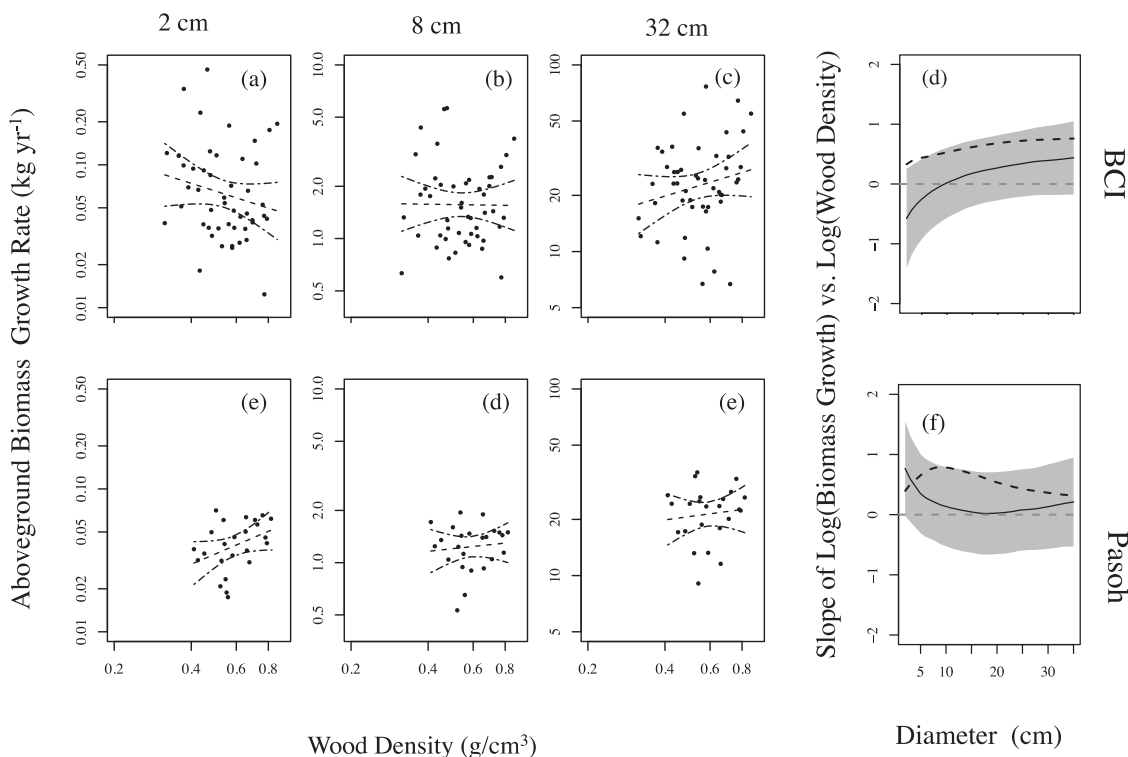


**FIGURE 4** Relationships of species-specific aboveground biomass growth rate versus wood density vary with reference diameter and between BCI and Pasoh, as shown in scatterplots of biomass growth rate versus wood density at 2 cm diameter (a, e), 8 cm diameter (b, d), and 32 cm diameter (c, g). The slopes of the relationship between log(biomass growth rate) and log(wood density) are plotted against diameter (d, h), where the black line shows the empirical slopes, and the dashed gray line shows the slope predicted from the null hypothesis that biomass growth is constant with wood density, and the dashed black line shows the slope predicted by the alternative hypothesis that biomass growth scales with crown area. The empirical slopes are not significantly different than the slope values predicted from the null hypothesis at any reference diameter (95% confidence intervals are shaded in gray behind the lines).

and high wood density functional group < 7 cm in diameter at BCI, and slightly higher in a high wood density functional group from 7 to 30 cm in diameter.

In contrast, we compared observed slopes of relationships between wood density and diameter growth with slopes predicted from a null hypothesis that aboveground biomass growth does not vary with wood density, and found evidence for slower biomass growth in trees with high wood density < 13 cm in diameter at BCI, and equal biomass growth with wood density in trees 13–35 cm in diameter at BCI and all tree sizes at Pasoh. This demonstrates that comparing observed relationships with those predicted from null hypotheses can guide nuanced interpretations of functional trait relationships. A similar approach has been applied previously to understand the strong interrelationships among mass-normalized leaf traits, which has been designated the ‘leaf economics spectrum’ (Wright, Reich, Westoby, & Ackerly, 2004). Osnas, Lichstein, Reich, and Pacala (2013) compared empirical relationships among mass-normalized leaf traits with theoretical relationships predicted from a null model that assumed no relationship among area-normalized leaf traits. The authors found that the slopes derived from the null model can almost reproduce the empirical relationships among the mass-normalized leaf traits (Lloyd, Bloomfield, Domingues, & Farquhar, 2013; Osnas et al., 2013), thus

calling into question the biological significance of these relationships. Nonetheless, both mass-normalized and area-normalized leaf traits can provide useful insights for different purposes (Poorter, Lambers, & Evans, 2014). In our example of wood density and tree trunk growth rates, we showed that wood density is not negatively related to growth when growth rates are measured on a mass basis, except for small trees at BCI. Furthermore, we argue that mass growth rates are the more ecologically relevant measure of tree trunk growth, because they are more directly related to whole-tree carbon gain than diameter growth rates.

### 5.3 | Implications

Wood density is a key parameter in ecosystem models that use plant functional types to predict the response of the biosphere to global change (Sitch et al., 2008; Weng et al., 2015). These models often assume that wood density influences growth through the higher biomass cost of each diameter increment, and our results support this model assumption (Falster, Brännström, Dieckmann, & Westoby, 2011; Kazmierczak, Wiegand, & Huth, 2014; Moorcroft et al., 2001). Our results also have applied implications for forest carbon sequestration efforts (e.g., Angelsen & Rudel, 2013). We found that aboveground

biomass growth and wood density were uncorrelated in trees > 13 cm in diameter (Figure 4). This suggests that reforestation projects seeking to maximize carbon stocks (Pichancourt, Firn, Chades, & Martin, 2014; Shimamoto, Botosso, & Marques, 2014) should focus on species with high wood density, which accumulate equal amounts of carbon and live longer, even if these species grow more slowly in diameter (Kraft et al., 2010; Muller-Landau et al., 2006; Wright et al., 2010).

## ACKNOWLEDGMENTS

The BCI forest dynamics research project was founded by S. P. Hubbell and R. B. Foster and is now managed by R. Condit, S. Lao and R. Perez under the Center for Tropical Forest Science and the Smithsonian Tropical Research in Panama. Numerous organizations have provided funding, principally the U.S. National Science Foundation, and hundreds of field workers have contributed. The 50-ha Forest Dynamics Plot at Pasoh is a collaborative project of the Forest Research Institute Malaysia (FRIM), the National Institute for Environmental Studies, Japan (NIES) and the Center for Tropical Forest Science–Arnold Arboretum Asia Program, Harvard University (CTFS-AA). We acknowledge all people who are related to the Global Wood Density Database.

## DATA ACCESSIBILITY

Demography data from the BCI 50-ha plot is available by request on the Center for Tropical Forest Science Website (<http://ctfs.si.edu/webatlas/datasets/bci/>). Allometry data and demographic data from Pasoh are not publicly available; requests can be directed to the relevant coauthors (H. C. Muller-Landau and S. J. Wright for BCI allometry and wood density data; Y. Iida and M. Visser for Pasoh allometry data; and C. Fletcher and A. R. Kassim for the Pasoh demographic data. Wood density data from 298 out of 336 species from Pasoh are available through the global wood density database (Zanne et al., 2009).

## ORCID

Emily J. Francis  <http://orcid.org/0000-0002-7123-781X>

## REFERENCES

- Aiba, M., & Nakashizuka, T. (2009). Architectural differences associated with adult stature and wood density in 30 temperate tree species. *Functional Ecology*, 23, 265–260.
- Angelsen, A., & Rudel, T. K. (2013). Designing and implementing effective REDD+ policies: A forest transition approach. *Review of Environmental Economics and Policy*, 7, 91–113.
- Anten, N. P. R., & Schieving, F. (2010). The role of wood mass density and mechanical constraints in the economy of tree architecture. *The American Naturalist*, 175, 250–260.
- Augsburger, C. K., & Kelly, C. K. (1984). Pathogen mortality of tropical tree seedlings: Experimental studies of the effects of dispersal distance, seedling density, and light conditions. *Oecologia*, 61, 211–217.
- Bohman, S., & O'Brien, S. (2006). Allometry, adult stature, and regeneration requirement of 65 tree species on Barro Colorado Island. *Journal of Tropical Ecology*, 22, 123–136.
- Chave, J., Coomes, D., Jansen, S., Lewis, S. L., Swenson, N. G., & Zanne, A. E. (2009). Towards a worldwide wood economics spectrum. *Ecology Letters*, 12, 351–366.
- Chave, J., Muller-Landau, H. C., Baker, T. R., Easdale, T. A., ter Steege, H., & Webb, C. O. (2006). Regional and phylogenetic variation of wood density across 2456 neotropical tree species. *Ecological Applications*, 16, 2356–2367.
- Chave, J., Réjou-Méchain, M., Búrquez, A., Chidumayo, E., Colgan, M. S., Delitti, W. B., ... Vieilledent, G. (2014). Improved allometric models to estimate the aboveground biomass of tropical trees. *Global Change Biology*, 20, 3177–3190.
- Condit, R. (1998). *Tropical forest census plots: Methods and results from Barro Colorado Island, Panama, and a comparison with other plots*. Berlin, Germany: Springer-Verlag and RG Landes Company.
- Condit, R., Ashton, P., Bunyavejchewin, S., Dattaraja, H. S., Davies, S., Esufali, S., ... Zillio, T. (2006). The importance of demographic niches to tree diversity. *Science*, 313, 98–101.
- Falster, D. S., Brännström, Å., Dieckmann, U., & Westoby, M. (2011). Influence of four major plant traits on average height, leaf-area cover, net primary productivity, and biomass density in single-species forests: A theoretical investigation. *Journal of Ecology*, 99, 148–164.
- Hacke, U. G., Sperry, J. S., Pockman, W. T., Davis, S. W., & McCulloh, K. A. (2001). Trends in wood density and structure are linked to prevention of xylem implosion by negative pressure. *Oecologia*, 126, 457–461.
- Hérault, B., Bachelot, B., Poorter, L., Rossi, V., Bongers, F., Chave, J., ... Baraloto, C. (2011). Functional traits shape ontogenetic growth trajectories of rain forest tree species. *Journal of Ecology*, 99, 1431–1440.
- Hietz, P., Rosner, S., Hietz-Siefert, U., & Wright, S. J. (2017). Wood traits related to size and life history of trees in a Panamanian rainforest. *New Phytologist*, 213, 170–180.
- Hietz, P., Valencia, R., & Wright, S. J. (2013). Strong radial variation in wood density follows a uniform pattern in two neotropical rain forests. *Functional Ecology*, 27, 684–692.
- Iida, Y., Kohyama, T. S., Swenson, N. G., Su, S.-H., Chen, C.-T., Chiang, J.-M., & Sun, I.-F. (2014). Linking functional traits and demographic rates in a subtropical tree community: The importance of size dependency. *Journal of Ecology*, 102, 641–650.
- Iida, Y., Poorter, L., Sterck, F. J., Kassim, A. R., Kubo, T., Potts, M. D., & Kohyama, T. S. (2012). Wood density explains architectural differentiation across 145 co-occurring tropical tree species. *Functional Ecology*, 26, 274–282.
- Iida, Y., Poorter, L., Sterck, F., Kassim, A. R., Potts, M. D., & Kubo, T., & Kohyama, T. S. (2014). Linking size-dependent growth and mortality with architectural traits across 145 co-occurring tropical tree species. *Ecology*, 95, 353–363.
- Kazmierczak, M., Wiegand, T., & Huth, A. (2014). A neutral vs. non-neutral parametrizations of a physiological forest gap model. *Ecological Modelling*, 288, 94–102.
- King, D., Davies, A., Supardi, M., & Tan, S. (2005). Tree growth is related to light interception and wood density in two mixed dipterocarp forests of Malaysia. *Functional Ecology*, 19, 445–453.
- King, D. A., Davies, S. J., Tan, S., & Noor, N. (2006). The role of wood density and stem support costs in the growth and mortality of tropical trees. *Journal of Ecology*, 94, 670–680.
- Kraft, N., Metz, M., Condit, R., & Chave, J. (2010). The relationship between wood density and mortality in a global tropical forest data set. *New Phytologist*, 188, 1124–1136.
- Lichstein, J., Dushoff, J., Ogle, K., Chen, A., Purves, D., Caspersen, J., & Pacala, S. W. (2010). Unlocking the forest inventory data: Relating

- individual tree performance to unmeasured environmental factors. *Ecological Applications*, 20, 684–699.
- Lloyd, J., Bloomfield, K., Domingues, T., & Farquhar, G. (2013). Photosynthetically relevant foliar traits correlating better on a mass vs. an area basis: Of ecophysiological relevance or just a case of mathematical imperatives and statistical quicksand? *New Phytologist*, 199, 311–321.
- Manokaran, N., Quah, E. S., Ashton, P., LaFrankie, J. V., Supardi, M., Ahmad, W. M. S. W., & Okuda, T. (2004). Pasoh forest dynamics plot, Peninsular Malaysia. In E. C. Losos & E. G. Leigh (Eds.), *Tropical forest diversity and dynamism: Findings from a large-scale plot network* (pp. 585–598). Chicago, IL: Chicago University Press.
- Moorcroft, P. R., Hurr, G. C., & Pacala, S. W. (2001). A method for scaling vegetation dynamics: The ecosystem demography model (ED). *Ecological Monographs*, 71, 557–586.
- Muller-Landau, H. C. (2004). Interspecific and inter-site variation in wood specific gravity of tropical trees. *Biotropica*, 36, 20–32.
- Muller-Landau, H. C., Condit, R. S., Chave, J., Thomas, S. C., Bohlman, S. A., Bunyavejchewin, S., ... Ashton, P. (2006). Testing metabolic ecology theory for allometric scaling of tree size, growth and mortality in tropical forests. *Ecology Letters*, 9, 575–588.
- Nascimento, H. E. M., Laurance, W. F., Condit, R., Laurance, S. G., Angelo, S., & Andrade, A. C. (2005). Demographic and life-history correlates for Amazonian trees. *Journal of Vegetation Science*, 16, 625–634.
- Osnas, J. L. D., Lichstein, J. W., Reich, P. B., & Pacala, S. W. (2013). Global leaf trait relationships: Mass, area, and the leaf economics spectrum. *Science*, 340, 741–744.
- Philpson, C. D., Dent, D. H., O'Brien, M. J., Chamagne, J., Dzikiffi, D., Nilus, R., & Hector, A. (2014). A trait-based trade-off between growth and mortality: Evidence from 15 tropical tree species using size-specific relative growth rates. *Ecology and Evolution*, 4, 3675–2688.
- Pichancourt, J. B., Firn, J., Chades, I., & Martin, T. G. (2014). Growing biodiverse carbon-rich forests. *Global Change Biology*, 20, 382–393.
- Poorter, H., Lambers, H., & Evans, J. R. (2014). Trait correlation networks: A whole-plant perspective on the recently criticized leaf economic spectrum. *New Phytologist*, 201, 378–382.
- Poorter, L., McDonald, I., Alarcón, A., Fichtler, E., Licona, J., Peña-Claros, M., ... Sass-Klaassen, U. (2010). The importance of wood traits and hydraulic conductance for the performance and life history strategies of 42 rainforest tree species. *New Phytologist*, 185, 481–492.
- Poorter, L., Wright, S. J., Paz, H., Ackerly, D. D., Condit, R., Ibarra-Manríquez, G., ... Wright, I. J. (2008). Are functional traits good predictors of demographic rates? Evidence from five neotropical forests. *Ecology*, 89, 1908–1920.
- Quesada, C. A., Phillips, O. L., Schwarz, M., Czimczik, C. I., Baker, T. R., Patiño, S., ... Lloyd, J. (2012). Basin-wide variations in Amazon forest structure and function are mediated by both soils and climate. *Biogeosciences*, 9, 2203–2246.
- Reich, P. B., Wright, I. J., Cavender-Bares, J. M., Craine, J., Oleksyn, J., Westoby, M., & Walters, M. B. (2003). The evolution of plant functional variation: Traits, spectra, and strategies. *International Journal of Plant Sciences*, 164, S143–S164.
- Rüger, N., Wirth, C., Wright, S. J., & Condit, R. (2012). Functional traits explain light and size response of growth rates in tropical tree species. *Ecology*, 93, 2626–2636.
- Schnitzer, S. A., & Carson, W. P. (2010). Lianas suppress tree regeneration and diversity in treefall gaps. *Ecology Letters*, 13, 849–857.
- Shimamoto, C. Y., Botosso, P. C., & Marques, M. C. M. (2014). How much carbon is sequestered during the restoration of tropical forests? Estimates from tree species in the Brazilian Atlantic forest. *Forest Ecology and Management*, 329, 1–9.
- Sitch, S., Huntingford, C., Gedney, N., Levy, P. E., Lomas, M., Piao, S. L., ... Woodward, F. I. (2008). Evaluation of the terrestrial carbon cycle, future plant geography and climate-carbon cycle feedbacks using five Dynamic Global Vegetation Models (DGVMs). *Global Change Biology*, 14, 2015–2039.
- Sterck, F. J., Van Gelder, H. A., & Poorter, L. (2006). Mechanical branch constraints contribute to life-history variation across tree species in a Bolivian forest. *Journal of Ecology*, 94, 1192–1200.
- Visser, M. D. (2016). *Trade-offs, enemies & dispersal: Cross-scale comparisons on tropical tree populations*. Nijmegen, The Netherlands: Radboud University.
- Visser, M. D., Bruijning, M., Wright, S. J., Muller-Landau, H. C., Jongejans, E., Comita, L. S., & de Kroon, H. (2016). Functional traits as predictors of vital rates across the life cycle of tropical trees. *Functional Ecology*, 30, 168–180.
- Weng, E. S., Malyshev, S., Lichstein, J. W., Farrior, C. E., Dybzinski, R., Zhang, T., ... Pacala, S. W. (2015). Scaling from individual trees to forests in an Earth system modeling framework using a mathematically tractable model of height-structured competition. *Biogeosciences*, 12, 2655–2694.
- Westoby, M., & Wright, I. J. (2006). Land-plant ecology on the basis of functional traits. *Trends in Ecology and Evolution*, 21, 261–268.
- Wright, I. J., Reich, P. B., Westoby, M., Ackerly, D. D. (2004). The worldwide leaf economics spectrum. *Nature*, 428, 821–827.
- Wright, S. J., Kitajima, K., Kraft, N. J. B., Reich, P. B., Wright, I. J., Bunker, D. E., ... Zanne, A. E. (2010). Functional traits and the growth-mortality trade-off in tropical trees. *Ecology*, 91, 3664–3674.
- Wyckoff, P. H., & Clark, J. S. (2005). Tree growth prediction using size and exposed crown area. *Canadian Journal of Forest Research*, 35, 13–20.
- Yoda, K. (1974). Three-dimensional distribution of light intensity in a tropical rain forest of West Malaysia. *Japanese Journal of Ecology*, 24, 247–254.
- Zanne, A. E., Lopez-Gonzalez, G., Coomes, D. A., Ilic, J., Jansen, S., Lewis, S. L., ... Chave, J. (2009). Data from: Towards a worldwide wood economics spectrum. Dryad Digital Repository. <http://dx.doi.org/10.5061/dryad.234>

## BIOSKETCH

EMILY J. FRANCIS received a BA degree in Ecology and Evolutionary Biology from Princeton University in 2013 and is currently pursuing a PhD in Earth System Science at Stanford University. Her research interests encompass the impacts of global change on tree diversity and forest carbon stocks in temperate and tropical forests.

## SUPPORTING INFORMATION

Additional Supporting Information may be found online in the supporting information tab for this article.

**How to cite this article:** Francis EJ, Muller-Landau HC, Wright SJ, et al. Quantifying the role of wood density in explaining interspecific variation in growth of tropical trees. *Global Ecol Biogeogr.* 2017;26:1078–1087. <https://doi.org/10.1111/geb.12604>

## Appendix S1. Full details on the derivation of the relationships of growth rates with wood density under the null and alternative hypotheses

### Derivation for the null hypothesis

We start from the following assumptions:

(1) Biomass at a given diameter,  $A(D)$ , is proportional to the product of wood density, basal area, and height (Chave et al. 2014), and thus can be written

$$M(D) = c\rho D^2 H(D)$$

(2) Biomass growth rate,  $\frac{dM}{dt}$ , depends only on diameter (and is independent of wood density):

$$\frac{dM}{dt} = g(D)$$

(3) Height is independent of wood density and is a piecewise power function of diameter (that is, log of height is a piecewise linear function of log of diameter), so that we can write

$$H(D) = \tilde{a}D^{\tilde{b}}$$

where  $\tilde{a}$  and  $\tilde{b}$  are the coefficients of the power function for diameter. Note that the independence of height with respect to wood density means specifically that the log-log slope of height at a given diameter vs. wood density is zero; this is the assumption we test in our empirical analyses.

It follows that the log of biomass at a given diameter is linearly related to the log of wood density, with a slope of one:

$$\log(M(D)) = \log(cD^2 H(D)) + \log(\rho)$$

To derive the expected diameter growth rate, we invoke the chain rule:

$$\frac{dD}{dt} = \frac{dD}{dM} \frac{dM}{dt}$$

Thus, we need to solve for the derivative of diameter with respect to biomass,  $\frac{dD}{dM}$ . Given the very general assumptions we make about the form of the height allometry, there is no exact analytical solution for this derivative. (If we assume that height is a simplepower function of diameter, then there is an analytical solution.) Fortunately, because we are specifically interested in comparing diameter growth rates across species at any given diameter,  $\tilde{D}$ , that is, in  $\left. \frac{dD}{dt} \right|_{D=\tilde{D}}$ , we do not need a generalized form of this derivative, but only its value in a region for  $D$  close to  $\tilde{D}$ , which we denote  $\left. \frac{dD}{dM} \right|_{D=\tilde{D}}$ .

We can approximate the derivative of diameter with respect to biomass in the region around any particular diameter,  $\tilde{D}$ , using a Taylor series expansion (for simplicity, in the main text we assume that  $D$  and  $\tilde{D}$  are equivalent).

$$M(\tilde{D} + \Delta D) \approx M(\tilde{D}) + \Delta D \left. \frac{dM}{dD} \right|_{D=\tilde{D}}$$

$$M(\tilde{D} + \Delta D) - M(\tilde{D}) \approx \Delta D \left. \frac{dM}{dD} \right|_{D=\tilde{D}}$$

$$\frac{dM}{dD} = c\rho D^2 \frac{dH}{dD} + 2c\rho DH(D) = c\rho D \left( D \frac{dH}{dD} + 2H(D) \right)$$

Given our assumption

$$H(D) = \tilde{\alpha} D^{\tilde{b}}$$

we then have

$$\left. \frac{dH}{dD} \right|_{D=\tilde{D}} = \tilde{\alpha} \tilde{b} \tilde{D}^{\tilde{b}-1}$$

and thus

$$\left. \frac{dM}{dD} \right|_{D=\tilde{D}} = c\rho \tilde{D} (\tilde{D} \tilde{\alpha} \tilde{b} \tilde{D}^{\tilde{b}-1} + 2\tilde{\alpha} \tilde{D}^{\tilde{b}})$$

$$\left. \frac{dM}{dD} \right|_{D=\tilde{D}} = c\tilde{\alpha} (\tilde{b} + 2) \rho \tilde{D}^{\tilde{b}+1}$$

$$M(\tilde{D} + \Delta D) - M(\tilde{D}) \approx \Delta D \left. \frac{dM}{dD} \right|_{D=\tilde{D}} = \Delta D c\tilde{\alpha} (\tilde{b} + 2) \rho \tilde{D}^{\tilde{b}+1}$$

$$\frac{\Delta D}{M(\tilde{D} + \Delta D) - M(\tilde{D})} \approx \frac{\Delta D}{\Delta D c\tilde{\alpha} (\tilde{b} + 2) \rho \tilde{D}^{\tilde{b}+1}}$$

$$\left. \frac{dD}{dM} \right|_{D=\tilde{D}} \approx \frac{1}{c\tilde{\alpha} (\tilde{b} + 2) \tilde{D}^{\tilde{b}+1} \rho^{-1}}$$

We can substitute height back into the equation to obtain

$$\left. \frac{dD}{dM} \right|_{D=\tilde{D}} \approx \frac{1}{c(\tilde{b} + 2) \tilde{D} H(\tilde{D})} \rho^{-1}$$

We can then use the chain rule to solve for the diameter growth rate:

$$\left. \frac{dD}{dt} \right|_{D=\tilde{D}} = \left. \frac{dD}{dM} \right|_{D=\tilde{D}} \left. \frac{dM}{dt} \right|_{D=\tilde{D}} \approx \frac{1}{c(\tilde{b} + 2) \tilde{D} H(\tilde{D})} \rho^{-1} g(\tilde{D})$$

$$\log\left(\frac{dD}{dt}\Big|_{D=\bar{D}}\right) \approx \log\left(\frac{g(\bar{D})}{c(\bar{b} + 2)\bar{D}H(\bar{D})}\right) - \log \rho$$

Thus, the relationship between the log of diameter growth rate at a given diameter and log of wood density is linear, with an intercept equal to the first term on the right-hand side, and a slope equal to negative one (and more generally, to the negative of the power of wood density in the biomass equation, as can be seen by doing the parallel derivation with a correspondingly altered biomass equation).

### Derivation for the alternative hypothesis

We start from the assumptions

$$M(D) = c\rho D^2 H(D)$$

$$\frac{dM}{dt} = kC(D)$$

$$C(D) = \rho^r f(D)$$

$$H(D) = \tilde{\alpha} D^{\bar{b}}$$

Note that this means that the log-log slope relating crown area at a given diameter to wood density is  $r$ :

$$\log(C|_{D=\bar{D}}) = \log(f(\bar{D})) + r \log \rho$$

Then

$$\frac{dM}{dt} = k\rho^r f(D)$$

$$\frac{dM}{dt}\Big|_{D=\bar{D}} \approx k\rho^r f(\bar{D})$$

$$\log\left(\frac{dM}{dt}\Big|_{D=\bar{D}}\right) \approx \log(kf(\bar{D})) + r \log \rho$$

$$\frac{dD}{dt}\Big|_{D=\bar{D}} = \frac{dD}{dM}\Big|_{D=\bar{D}} \frac{dM}{dt}\Big|_{D=\bar{D}} \approx \frac{1}{c(\bar{b} + 2)\bar{D}H(\bar{D})} \rho^{-1} k\rho^r f(\bar{D})$$

$$\frac{dD}{dt} = \frac{k}{c(\tilde{b} + 2)\tilde{D}H(\tilde{D})} \rho^{r-1} f(\tilde{D})$$

$$\log\left(\frac{dD}{dt}\Big|_{D=\tilde{D}}\right) = \log\left(\frac{kf(\tilde{D})}{c(\tilde{b} + 2)\tilde{D}H(\tilde{D})}\right) + (r - 1) \log \rho$$

Thus, the log of the diameter growth rate at a given diameter is expected to be linearly related to the log of wood density, with a slope of  $r - 1$ , where  $r$  is the log-log slope relating crown area at a given diameter to wood density.

SUPPORTING INFORMATION FOR:

“PLANT: A PACKAGE FOR MODELLING FOREST TRAIT ECOLOGY & EVOLUTION”

## DESCRIPTION OF THE FF16 PHYSIOLOGICAL MODEL

DANIEL S. FALSTER<sup>†</sup>, RICHARD G. FITZJOHN, ÅKE BRÄNNSTRÖM, ULF DIECKMANN, AND  
MARK WESTOBY

<sup>†</sup>Department of Biological Sciences, Macquarie University, Sydney, Australia

daniel.falster@mq.edu.au, rich.fitzjohn@gmail.com

---

## CONTENTS

<b>1</b>	<b>Introduction</b>	<b>1</b>
<b>2</b>	<b>Growth</b>	<b>2</b>
2.1	Leaf photosynthesis . . . . .	2
2.2	Mass production . . . . .	3
2.3	Height growth . . . . .	3
2.4	Diameter growth . . . . .	3
<b>3</b>	<b>Functional-balance model for allocation</b>	<b>4</b>
3.1	Leaf area . . . . .	4
3.2	Vertical distribution of leaf area . . . . .	4
3.3	Sapwood mass . . . . .	5
3.4	Bark mass . . . . .	5
3.5	Root mass . . . . .	5
<b>4</b>	<b>Seed production</b>	<b>5</b>
<b>5</b>	<b>Mortality</b>	<b>5</b>
<b>6</b>	<b>Hyper-parameterisation of physiological model via traits</b>	<b>6</b>
6.1	Leaf mass per unit area . . . . .	6
6.2	Wood density . . . . .	7
6.3	Seed mass . . . . .	7
6.4	Nitrogen per unit leaf area . . . . .	7
<b>7</b>	<b>Tables</b>	<b>9</b>

## 1 INTRODUCTION

This document outlines the core physiological model used in the PLANT package. This model has primarily been developed elsewhere, in particular in Falster *et al.* (2011). The model’s equations are presented here not as original findings, but rather so that users can understand the full system of equations being solved within PLANT.

The purpose of a physiological model in `PLANT` is to take a plant's current size, light environment, and physiological parameters as inputs, and return its growth, mortality, and fecundity rates. In the FF16 physiological model, these vital rates are all derived from the rate at which living biomass is produced by the plant, which in turn is calculated based on well-understood physiology (Fig. 1). Various physiological parameters influence demographic outcomes. Varying these parameters allows accounting for species differences, potentially via traits (see last section). Tables 1, 3, 4 summarize the units and definitions of all variables, parameters, and hyper-parameters used in the material below.

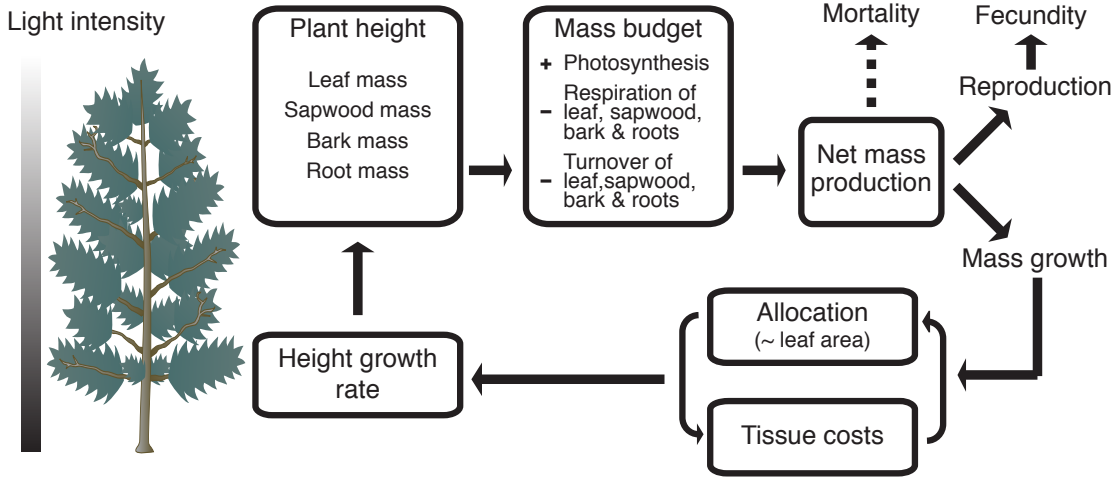


FIGURE 1: Physiological model in `PLANT`, giving demographic rates on the basis of its traits, size, and light environment, as functions of net mass production. The dashed arrow towards mortality indicates that, although the mortality rate is assumed to depend on mass production, no mass is actually allocated there. Figure adapted from Falster *et al.* (2011) and Falster *et al.* (2015).

## 2 GROWTH

### 2.1 Leaf photosynthesis

We denote by  $p(x, E)$  the gross rate of leaf photosynthesis per unit leaf area within the canopy of a plant with traits  $x$  at light level  $E(z)$ , where  $z$  is height within the canopy. We assume a relationship of the form

$$p(x, E(z)) = \frac{\alpha_{p1}}{E(z) + \alpha_{p2}}, \quad (1)$$

for the average of  $p$  across the year. The parameters  $\alpha_{p1}$  and  $\alpha_{p2}$  are derived from a detailed leaf-level model and measure, respectively, maximum annual photosynthesis and the light levels at 50% of this maximum. The average rate of leaf photosynthesis across the plant is then

$$\bar{p}(x, H, E_a) = \int_0^H p(x, E_a(z)) q(z, H) dz, \quad (2)$$

where  $q(z, H)$  is the vertical distribution of leaf area with respect to height  $z$  (Eq. 13).

### 2.2 Mass production

The amount of biomass available for growth,  $dB/dt$ , is given by the difference between income (total photosynthetic rate) and losses (respiration and turnover) within the plant (Mäkelä, 1997; Thornley & Cannell, 2000; Falster *et al.*, 2011),

$$\underbrace{\frac{dB}{dt}}_{\text{net biomass production}} = \underbrace{\alpha_{\text{bio}}}_{\text{mass per C}} \underbrace{\alpha_y}_{\text{yield}} \left( \underbrace{A_1 \bar{p}}_{\text{photosynthesis}} - \underbrace{\sum_{i=l,b,s,r} M_i r_i}_{\text{respiration}} \right) - \underbrace{\sum_{i=l,b,s,r} M_i k_i}_{\text{turnover}}. \quad (3)$$

Here,  $M$ ,  $r$ , and  $k$  refer to the mass, maintenance respiration rate, and turnover rate of different tissues, denoted by subscripts  $l = \text{leaves}$ ,  $b = \text{bark}$ ,  $s = \text{sapwood}$ , and  $r = \text{roots}$ .  $\bar{p}$  is the assimilation rate of  $\text{CO}_2$  per unit leaf area,  $\alpha_y$  is yield (i.e., the fraction of assimilated carbon fixed in biomass, with the remaining fraction being lost as growth respiration; this comes in addition to the costs of maintenance respiration), and  $\alpha_{\text{bio}}$  is the amount of biomass per unit carbon fixed. Gross photosynthetic production is proportional to leaf area,  $A_1 = M_1/\phi$ , where  $\phi$  is leaf mass per area. The total mass of living tissues is  $M_a = M_l + M_b + M_s + M_r$ .

### 2.3 Height growth

The key measure of growth required by the demographic model is the rate of height growth, denoted  $g(x, H, E_a)$ . To model height growth requires that we translate mass production into height increment, accounting for the costs of building new tissues, allocation to reproduction, and architectural layout. Using the chain rule, height growth can be decomposed into a product of physiologically relevant terms (Falster *et al.*, 2011),

$$g(x, H, E_a) = \frac{dH}{dt} = \frac{dH}{dA_1} \times \frac{dA_1}{dM_a} \times \frac{dM_a}{dB} \times \frac{dB}{dt}. \quad (4)$$

The first factor,  $dH/dA_1$ , is the growth in plant height per unit growth in total leaf area – accounting for the architectural strategy of the plant. Some species tend to leaf out more than grow tall, while other species emphasise vertical extension.

The second factor,  $dA_1/dM_a$ , accounts for the marginal cost of deploying an additional unit of leaf area, including construction of the leaf itself and various support structures. As such,  $dA_1/dM_a$  can itself be expressed as a sum of construction costs per unit leaf area,

$$\frac{dA_1}{dM_a} = \left( \frac{dM_l}{dA_1} + \frac{dM_s}{dA_1} + \frac{dM_b}{dA_1} + \frac{dM_r}{dA_1} \right)^{-1}. \quad (5)$$

The third factor,  $dM_a/dB$ , is the fraction of net biomass production (Eq. 3) that is allocated to growth rather than reproduction or storage. In the FF16 physiological model, we let this growth fraction decrease with height according to the function

$$\frac{dM_a}{dB}(H) = 1 - \frac{\alpha_{f1}}{1 + \exp(\alpha_{f2}(1 - H/H_{\text{mat}}))}, \quad (6)$$

where  $\alpha_{f1}$  is the maximum possible allocation (0 – 1) and  $\alpha_{f2}$  determines the sharpness of the transition (Falster *et al.*, 2011).

#### 2.4 Diameter growth

Analogously, the growth in basal area  $A_{st}$  can be expressed as the sum of growth in sapwood, bark, and heartwood areas ( $A_s$ ,  $A_b$ , and  $A_h$ , respectively),

$$\frac{dA_{st}}{dt} = \frac{dA_b}{dt} + \frac{dA_s}{dt} + \frac{dA_h}{dt}.$$

Applying the chain rule, we derive an equation for basal area growth that contains many of the same elements as Eq. 4,

$$\frac{dA_{st}}{dt} = \left( \frac{dA_s}{dA_1} + \frac{dA_b}{dA_1} \right) \times \frac{dA_1}{dM_a} \times \frac{dM_a}{dB} \times \frac{dB}{dt} + \frac{dA_h}{dt}. \quad (7)$$

Diameter growth is then given by the geometric relationship between stem diameter  $D$  and  $A_{st}$ ,

$$\frac{dD}{dt} = (\pi A_{st})^{-0.5} \frac{dA_{st}}{dt}. \quad (8)$$

### 3 FUNCTIONAL-BALANCE MODEL FOR ALLOCATION

Here we describe an allometric model linking to a plant's height its various other size dimensions required by most ecologically realistic vegetation models (i.e., the masses of leaves, sapwood, bark, and fine roots). This approach allows us to track only the plant's height, while still accounting for the mass needs to build leaves, roots, and stems. The growth rates of various tissues can then also be derived (Table 2).

#### 3.1 Leaf area

Based on empirically observed allometry (Falster *et al.*, 2011), we assume an allometric power-law scaling relationship between the accumulated leaf area of a plant and its height,

$$H = \alpha_{11} \left( A_1 \text{m}^{-2} \right)^{\alpha_{12}}. \quad (9)$$

This relationship is normalised around a leaf area of  $1\text{m}^2$ .

#### 3.2 Vertical distribution of leaf area

We follow the model of Yokozawa & Hara (1995) describing the vertical distribution of leaf area within the crowns of individual plants. This model can account for a variety of canopy profiles through a single parameter  $\eta$ . Setting  $\eta = 1$  results in a conical canopy, as seen in many conifers, while higher values, e.g.,  $\eta = 12$ , give a top-heavy canopy profile similar to those seen among angiosperms. We denote by  $A_{s,z}$  the sapwood area at height  $z$  within the plant, by  $q(z, H)$  the vertical distribution of leaf area of leaf area with respect to height  $z$ , and by  $Q(z, H)$  the cumulative fraction of a plant's leaves above height  $z$ . As defined previously,  $A_s$  is the sapwood area at the base of the plant. Following Yokozawa & Hara (1995), we assume a relationship between  $A_{s,z}$  and height such that

$$\frac{A_{s,z}}{A_s} = \left( 1 - \left( \frac{z}{H} \right)^\eta \right)^2. \quad (10)$$

We also assume that each unit of leaf area is supported by a fixed area  $\theta$  of sapwood (in agreement with the pipe model; Shinozaki *et al.*, 1964), so that the total canopy area of a plant

relates to its basal sapwood area  $A_s$ ,

$$A_s = \theta A_1. \quad (11)$$

The pipe model is assumed to hold within individual plants, as well as across plants of different size. It follows that

$$Q(z, H) = \left(1 - \left(\frac{z}{H}\right)^\eta\right)^2. \quad (12)$$

Differentiating with respect to  $z$  then yields a solution for the probability density of leaf area as a function of height,

$$q(z, H) = 2\frac{\eta}{H} \left(1 - \left(\frac{z}{H}\right)^\eta\right) \left(\frac{z}{H}\right)^{\eta-1}. \quad (13)$$

### 3.3 Sapwood mass

Integrating  $A_{s,z}$  yields the total mass of sapwood in a plant,

$$M_s = \rho \int_0^H A_{s,z} dz = \rho A_s H \eta_c, \quad (14)$$

where  $\eta_c = 1 - \frac{2}{1+\eta} + \frac{1}{1+2\eta}$  (Yokozawa & Hara, 1995). Substituting from Eq. 11 into Eq. 14 then gives an expression for sapwood mass as a function of leaf area and height,

$$M_s = \rho \eta_c \theta A_1 H. \quad (15)$$

### 3.4 Bark mass

Bark and phloem tissue are modelled using an analogue of the pipe model, leading to a similar equation as that for sapwood mass (Eq. 15). The cross-section area of bark per unit leaf area is assumed to be a constant fraction  $\alpha_{b1}$  of sapwood area per unit leaf area such that

$$M_b = \alpha_{b1} M_s. \quad (16)$$

### 3.5 Root mass

Also consistent with the pipe model, we assume a fixed ratio of root mass per unit leaf area,

$$M_r = \alpha_{r1} A_1. \quad (17)$$

Even though nitrogen and water uptake are not modelled explicitly, imposing a fixed ratio of root mass to leaf area ensures that approximate costs of root production are included in calculations of carbon budget.

## 4 SEED PRODUCTION

The rate of seed production,  $f(x, H, E_a)$ , is a direct function of the mass allocated to reproduction,

$$f(x, H, E_a) = \frac{\left(1 - \frac{dM_a}{dB}\right) \times \frac{dB}{dt}}{\omega + \alpha_{f3}}, \quad (18)$$

where  $\omega$  is the mass of the seed and  $\alpha_{f3}$  is the cost per seed of accessories, such as fruits, flowers, and dispersal structures. The function  $\frac{dM_a}{dB}$  is the fraction of  $\frac{dB}{dt}$  that is allocated to growth (from Eq. 6, while  $1 - \frac{dM_a}{dB}$  gives the fraction allocated to reproduction).

## 5 MORTALITY

Instantaneous rates of plant mortality are given by the sum of a growth-independent and a growth-dependent rate (Falster *et al.*, 2011; Moorcroft, Hurtt & Pacala, 2001),

$$d(x, H, E_a) = d_1(x, H) + d_G(x, H, E_a). \quad (19)$$

The growth-independent rate is taken to be constant, independent of plant performance, but potentially varying with species traits. The growth-dependent rate is assumed to decline exponentially with the rate of mass production per unit leaf area,

$$d_G(x, H, E_a) = \alpha_{dG1} \exp(-\alpha_{dG2} X), \quad (20)$$

where  $X = dB/dt/A_1$ . This relationship allows for plants to increase in mortality as their growth rate approaches zero, while allowing for species to differ in the parameters  $\alpha_{dG1}$  and  $\alpha_{dG2}$ .

We also require a function  $S_G(x', H_0, E_{a0})$  for plant survival through germination. For the demographic model to behave smoothly,  $S_G(x', H_0, E_{a0})/g(x, H_0, E_{a0})$  should approach zero as  $g(x, H_0, E_{a0})$  approaches zero. Following Falster *et al.* (2011), we use the function

$$S_G(x', H_0, E_{a0}) = \frac{1}{1 + X^2}, \quad (21)$$

where  $X = \alpha_{d0} \frac{A_1}{dB/dt}$  and  $\alpha_{d0}$  is a constant. Eq. 21 is consistent with Eq. 20, as both cause survival to decline with mass production.

## 6 HYPER-PARAMETERISATION OF PHYSIOLOGICAL MODEL VIA TRAITS

The FF16 physiological model includes default values for all needed parameters (Table 3). Species are known to vary considerably in many of these parameters, such as  $\phi$ ,  $\rho$ ,  $\nu$ , and  $\omega$ ; so by varying parameters one can account for species differences. When altering a parameter in the model, however, one must also consider whether there are trade-offs linking parameters.

PLANT allows for the hyper-parameterisation of the FF16 physiological model via plant functional traits: this enables simultaneous variation in multiple parameters in accordance with an assumed trade-off. In the FF16 physiological model, we implement the relationships described below. For more details, see `make_FF16_hyperpar.R`.

### 6.1 Leaf mass per unit area

The trait leaf mass per unit area, denoted by  $\phi$ , directly influences growth by changing  $dA_1/dM_a$ . In addition, we link  $\phi$  to the rate of leaf turnover, based on a widely observed scaling relationship from Wright *et al.* (2004),

$$k_1 = \beta_{k11} \left( \frac{\phi}{\phi_0} \right)^{-\beta_{k12}}.$$

This relationship is normalised around  $\phi_0$ , the global mean of  $\phi$ . This allows us to vary  $\beta_{k11}$  and  $\beta_{k12}$  without displacing the relationship from the observed mean.

We also vary the mass-based leaf respiration rate so that it stays constant per unit leaf area and varies with  $\phi$  and nitrogen per unit leaf area  $\nu$ , as empirically observed by Wright *et al.*

(2004),

$$r_1 = \frac{\beta_{1f4} v}{\phi}.$$

### 6.2 Wood density

The trait wood density, denoted by  $\rho$ , directly influences growth by changing  $dA_1/dM_a$ . In addition, we allow for  $\rho$  to influence the rate of growth-independent mortality,

$$d_I = \beta_{dI1} \left( \frac{\rho}{\rho_0} \right)^{-\beta_{dI2}},$$

and also the rate of sapwood turnover,

$$k_s = \beta_{ks1} \left( \frac{\rho}{\rho_0} \right)^{-\beta_{ks2}},$$

As for  $\phi$ , these relationships are normalized around  $\rho_0$ , the global mean of  $\rho$ . By default,  $\beta_{dI2}$  and  $\beta_{ks2}$  are set to zero, so these linkages only become present when these parameters are set to something other than their default values.

The rate of sapwood respiration per unit volume is assumed to be constant, so sapwood respiration per unit mass varies as

$$r_s = \frac{\beta_{rs1}}{\rho},$$

where  $\beta_{rs1}$  is a default rate per volume of sapwood. Similarly, the rate of bark respiration per unit mass varies as

$$r_b = \frac{\beta_{rb1}}{\rho},$$

with  $\beta_{rb1} = 2\beta_{rs1}$ .

### 6.3 Seed mass

Effects of the trait seed mass, denoted by  $\omega$ , are naturally embedded in the equation determining fecundity (Eq. 18) and the initial height of seedlings. In addition, we let the accessory cost per seed be a multiple of seed size,

$$\alpha_{f3} = \beta_{f1}\omega,$$

as empirically observed (Henary & Westoby, 2001).

### 6.4 Nitrogen per unit leaf area

Photosynthesis per unit leaf area and respiration rates per unit leaf mass (or area) are assumed to vary with leaf nitrogen per unit area,  $\nu$ . The calculation of respiration rates is already described above. To calculate the average annual photosynthesis for a leaf, we integrate the instantaneous rate per unit leaf area over the annual solar trajectory, using a rectangular-hyperbolic photosynthesis light response curve,

$$p(\nu, E) = \frac{1}{365d} \int_0^{365d} \frac{Y(t) + A_{\max} - \sqrt{(Y(t) + A_{\max})^2 - 4\beta_{1f2}Y(t)A_{\max}}}{2\beta_{1f2}} dt,$$

where

- $A_{\max}$  is the maximum photosynthetic capacity of the leaf,
- $\beta_{1f2}$  is the curvature of the light response curve,
- $Y(t) = \beta_{1f3}I(t)$  is the initial yield of the light response curve, with  $\beta_{1f3}$  being the quantum yield parameter,
- $I(t) = k_1 I_0(t) E$  is the intensity of light on the leaf surface, and
- $I_0(t)$  is light incident on a surface perpendicular to the sun's rays directly above the canopy at time  $t$ .

The profile of  $I_0(t)$  is given by a solar model adapted from [Ter Steege \(1997\)](#).

We allow for the maximum photosynthetic capacity of the leaf to vary with leaf nitrogen per unit area, as

$$A_{\max} = \beta_{1f1} \left( \frac{\nu}{\nu_0} \right)^{\beta_{1f5}}, \quad (22)$$

where  $\beta_{1f1}$  and  $\beta_{1f5}$  are constants. The relationship is normalized around  $\nu_0$ , the global mean of leaf nitrogen per unit area.

Values of  $p(\nu, E)$  are calculated across a range of values of  $E$ , and then an expression of the form in Eq. 1 is fitted to extract the parameters  $\alpha_{p1}$  and  $\alpha_{p2}$ , such that these become functions of  $\nu$ .

## 7 TABLES

TABLE 1: Key variables of the FF16 physiological model. For mass ( $M$ ), respiration ( $r$ ), and turnover ( $k$ ) variables, subscripts refer to any of the following tissues: l = leaves, b = bark, s = sapwood, r = roots, a = all living tissue. For area  $A$  variables, subscripts refer to any of the following: l = leaves, st = total stem cross-section, s = sapwood cross-section, b = bark cross-section, h = heartwood cross-section.

Symbol	Unit	Description
<b>Plant construction</b>		
$x$		Vector of traits for a species
$H_0$	m	Height of a seedling after germination
$H$	m	Height of a plant
$B$	kg	Biomass originating from parent plant
$M_i$	kg	Mass of tissue type $i$ retained on plant
$A_i$	m <sup>2</sup>	Surface area or area of cross-section of tissue type $i$
$q(z, H)$	m <sup>-1</sup>	Vertical distribution of leaf area across heights $z$ for a plant with height $H$
$Q(z, H)$		Fraction of leaf area above height $z$ for a plant with height $H$
<b>Mass production</b>		
$p, \bar{p}$	mol yr <sup>-1</sup> m <sup>-2</sup>	Photosynthetic rate per unit area
$r_i$	mol yr <sup>-1</sup> kg <sup>-1</sup>	Respiration rate per unit mass of tissue type $i$
$k_i$	yr <sup>-1</sup>	Turnover rate for tissue type $i$
<b>Environment</b>		
$a$	yr	Patch age
$E_a$		Profile of canopy openness within a patch of age $a$
$E_a(z)$		Canopy openness at height $z$ within a patch of age $a$
<b>Demographic outcomes</b>		
$g(x, H, E_a)$	m yr <sup>-1</sup>	Height growth rate of a plant with traits $x$ and height $H$ in the light environment $E_a$ in a patch of age $a$
$f(x, H, E_a)$	yr <sup>-1</sup>	Seed production rate of a plant with traits $x$ and height $H$ in the light environment $E_a$ in a patch of age $a$
$d(x, H, E_a)$	yr <sup>-1</sup>	Instantaneous mortality rate of a plant with traits $x$ and height $H$ in the light environment $E_a$ in a patch of age $a$
$S_G(x, H_0, E_{a0})$		Probability that a seed germinates successfully

TABLE 2: Equations of the allometric growth model implemented within the FF16 physiological model, based on functional-balance assumptions (see text for details). The key assumptions allocation model are listed in (a), under “Function”. From these assumptions, allocation functions are derived for tissue areas and tissue masses (b). Also the growth rate of each tissue type can be expressed as a function of the growth rate of leaf area. For mass ( $M$ ), respiration ( $r$ ), and turnover ( $k$ ) variables, subscripts refer to any of the following tissues: l = leaves, b = bark, s = sapwood, r = roots, a = all living tissue. For area  $A$  variables, subscripts refer to any of the following: l = leaves, st = total stem cross-section, s = sapwood cross-section, b = bark cross-section, h = heartwood cross-section.

Variable	Function	Allocation	Growth rate
<b>(a) Assumed relationships with leaf area</b>			
Height	$H = \alpha_{11} (A_1 \text{ m}^{-2})^{\alpha_{12}}$	$\frac{dH}{dA_1} = \alpha_{12} \alpha_{11} (A_1 \text{ m}^{-2})^{\alpha_{12}-1}$	$\frac{dH}{dt} = \frac{dH}{dA_1} \frac{dA_1}{dt}$
Sapwood area	$A_s = \theta A_1$	$\frac{dA_s}{dA_1} = \theta$	$\frac{dA_s}{dt} = \frac{dA_s}{dA_1} \frac{dA_1}{dt}$
Bark area	$A_b = \alpha_{b1} \theta A_1$	$\frac{dA_b}{dA_1} = \alpha_{b1} \theta$	$\frac{dA_b}{dt} = \frac{dA_b}{dA_1} \frac{dA_1}{dt}$
<b>(b) Derived equations for mass of tissue</b>			
Leaf mass	$M_l = \phi A_1$	$\frac{dM_l}{dA_1} = \phi$	$\frac{dM_l}{dt} = \frac{dM_l}{dA_1} \frac{dA_1}{dt}$
Sapwood mass	$M_s = \rho \theta \eta_c A_1 H$	$\frac{dM_s}{dA_1} = \rho \theta \eta_c (H + A_1 \frac{dH}{dA_1})$	$\frac{dM_s}{dt} = \frac{dM_s}{dA_1} \frac{dA_1}{dt}$
Bark mass	$M_b = \alpha_{b1} \rho \theta \eta_c A_1 H$	$\frac{dM_b}{dA_1} = \alpha_{b1} \rho \theta \eta_c (H + A_1 \frac{dH}{dA_1})$	$\frac{dM_b}{dt} = \frac{dM_b}{dA_1} \frac{dA_1}{dt}$
Root mass	$M_r = \alpha_{r1} A_1$	$\frac{dM_r}{dA_1} = \alpha_{r1}$	$\frac{dM_r}{dt} = \frac{dM_r}{dA_1} \frac{dA_1}{dt}$

TABLE 3: Core parameters of the FF16 physiological model.

Description	Symbol	Unit	Code	Value
<b>Plant construction</b>				
Crown-shape parameter	$\eta$		eta	12
Leaf mass per area	$\phi$	$\text{kg m}^{-2}$	lma	0.1978791
Wood density	$\rho$	$\text{kg m}^{-3}$	rho	608
Sapwood area per unit leaf area	$\theta$		theta	0.0002141786
Height of plant with leaf area of $1\text{m}^2$	$\alpha_{11}$	m	a_l1	5.44
Exponent of relationship between height and leaf area	$\alpha_{12}$		a_l2	0.306
Root mass per unit leaf area	$\alpha_{r1}$	$\text{kg m}^{-2}$	a_r1	0.07
Ratio of bark area to sapwood area	$\alpha_{b1}$		a_b1	0.17
<b>Production</b>				
Leaf photosynthesis per area	$\alpha_{p1}$	$\text{mol yr}^{-1} \text{m}^{-2}$	a_p1	151.1778
Saturation of leaf photosynthesis per area	$\alpha_{p2}$		a_p2	0.2047162
Yield = fraction of carbon fixed converted into mass	$\alpha_y$		a_y	0.7
Biomass per mol carbon	$\alpha_{\text{bio}}$	$\text{kg mol}^{-1}$	a_bio	0.0245
Leaf respiration per mass	$r_l$	$\text{mol yr}^{-1} \text{kg}^{-1}$	r_l	198.4545
Fine-root respiration per mass	$r_r$	$\text{mol yr}^{-1} \text{kg}^{-1}$	r_r	217
Sapwood respiration per mass	$r_s$	$\text{mol yr}^{-1} \text{kg}^{-1}$	r_s	6.598684
Bark respiration per mass	$r_b$	$\text{mol yr}^{-1} \text{kg}^{-1}$	r_b	13.19737
Turnover rate for leaves	$k_l$	$\text{yr}^{-1}$	k_l	0.4565855
Turnover rate for sapwood	$k_s$	$\text{yr}^{-1}$	k_s	0.2
Turnover rate for bark	$k_b$	$\text{yr}^{-1}$	k_b	0.2
Turnover rate for fine roots	$k_r$	$\text{yr}^{-1}$	k_r	1
<b>Fecundity</b>				
Seed mass	$\omega$	kg	omega	0.000038
Height at maturation	$H_{\text{mat}}$	m	hmat	16.59587
Maximum allocation to reproduction	$\alpha_{f1}$		a_f1	1
Parameter determining rate of change in $r(x, m_l)$ around $H_{\text{mat}}$	$\alpha_{f2}$		a_f2	50
Accessory cost per seed	$\alpha_{f3}$	kg	a_f3	0.000114
<b>Mortality</b>				
Survival probability during dispersal	$S_D$		S_D	0.25
Parameter influencing survival through germination	$\alpha_{d0}$	$\text{kg yr}^{-1} \text{m}^{-2}$	a_d0	0.1
Intrinsic or growth-independent mortality	$d_I$	$\text{yr}^{-1}$	d_I	0.01
Baseline rate for growth-dependent mortality	$\alpha_{dG1}$	$\text{yr}^{-1}$	a_dG1	5.5
Risk coefficient for dry-mass production per unit leaf area in growth-dependent mortality	$\alpha_{dG2}$	$\text{yr m}^2 \text{kg}^{-1}$	a_dG2	20

TABLE 4: Parameters for hyper-parameterisation of the FF16 physiological model.

Description	Symbol	Unit	Code	Value
<b>Leaf turnover</b>				
Global average leaf mass per area	$\phi_0$	$\text{kg m}^{-2}$	lma_0	0.1978791
Rate of leaf turnover at average leaf mass per unit leaf area, $\phi_0$	$\beta_{kl1}$	$\text{yr}^{-1}$	B_kl1	0.4565855
Scaling exponent for $\phi$ in leaf turnover	$\beta_{kl2}$		B_kl2	1.71
<b>Sapwood turnover</b>				
Global average wood density	$\rho_0$	$\text{kg m}^{-3}$	rho_0	608
Rate of sapwood turnover at average wood density, $\rho_0$	$\beta_{ks1}$	$\text{yr}^{-1}$	B_ks1	0.2
Scaling exponent for $\rho$ in sapwood turnover	$\beta_{ks2}$		B_ks2	0
<b>Growth-independent mortality</b>				
Rate of instantaneous mortality at average wood density, $\rho_0$	$\beta_{dl1}$	$\text{yr}^{-1}$	B_dI1	0.01
Scaling exponent for wood density in intrinsic mortality	$\beta_{dl2}$		B_dI2	0
<b>Photosynthesis</b>				
Leaf nitrogen per unit leaf area	$\nu$	$\text{kg m}^{-2}$	narea	0.00187
Global average nitrogen per unit leaf area	$\nu_0$	$\text{kg m}^{-2}$	narea_0	0.00187
Potential $\text{CO}_2$ photosynthesis at average leaf nitrogen, $\nu_0$	$\beta_{lf1}$	$\text{mol d}^{-1} \text{m}^{-2}$	B_lf1	0.8273474
Curvature of light response curve	$\beta_{lf2}$		B_lf2	0.5
Quantum yield of leaf photosynthesis ( $\text{CO}_2$ per unit photosynthetically active radiation)	$\beta_{lf3}$		B_lf3	0.04
Scaling exponent for leaf nitrogen in maximum leaf photosynthesis	$\beta_{lf5}$		B_lf5	1
<b>Respiration</b>				
$\text{CO}_2$ respiration per unit leaf nitrogen	$\beta_{lf4}$	$\text{mol yr}^{-1} \text{kg}^{-1}$	B_lf4	21000
$\text{CO}_2$ respiration per unit sapwood volume	$\beta_{rs1}$	$\text{mol yr}^{-1} \text{m}^{-3}$	B_rs1	4012
$\text{CO}_2$ respiration per unit bark volume	$\beta_{rb1}$	$\text{mol yr}^{-1} \text{m}^{-3}$	B_rb1	8024
<b>Reproduction</b>				
Cost of seed accessories per unit seed mass	$\beta_{f1}$		B_f1	3

## REFERENCES

- Falster, D.S., Brännström, Å., Dieckmann, U. & Westoby, M. (2011) Influence of four major plant traits on average height, leaf-area cover, net primary productivity, and biomass density in single-species forests: a theoretical investigation. *Journal of Ecology*, **99**, 148–164.
- Falster, D.S., Brännström, Å., Westoby, M. & Dieckmann, U. (2015) Multi-trait eco-evolutionary dynamics explain niche diversity and evolved neutrality in forests. *bioRxiv*, p. 014605.
- Henery, M. & Westoby, M. (2001) Seed mass and seed nutrient content as predictors of seed output variation between species. *Oikos*, **92**, 479–490.
- Mäkelä, A. (1997) A carbon balance model of growth and self-pruning in trees based on structural relationships. *Forest Science*, **43**, 7–24.
- Moorcroft, P.R., Hurtt, G.C. & Pacala, S.W. (2001) A method for scaling vegetation dynamics: the Ecosystem Demography model (ED). *Ecological Monographs*, **71**, 557–586.
- Shinozaki, K., Yoda, K., Hozumi, K. & Kira, T. (1964) A quantitative analysis of plant form - the pipe model theory. I. Basic analyses. *Japanese Journal of Ecology*, **14**, 97–105.
- Ter Steege, H. (1997) *Winphot 5: a programme to analyze vegetation indices, light and light quality from hemispherical photographs*. Number 97-3 in Tropenbos Guyana Reports. Tropenbos Guyana Programme, Georgetown, Guyana.
- Thornley, J.H.M. & Cannell, M.G.R. (2000) Modelling the components of plant respiration: representation and realism. *Annals of Botany*, **85**, 55–67.
- Wright, I.J., Reich, P.B., Westoby, M., Ackerly, D., Baruch, Z., Bongers, F., Cavender-Bares, J., Chapin, F., Cornelissen, J., Diemer, M., Flexas, J., Garnier, E., Groom, P., Gulias, J., Hikosaka, K., Lamont, B., Lee, T., Lee, W., Lusk, C., Midgley, J., Navas, M.L., Niinemets, Ü., Oleksyn, J., Osada, N., Poorter, H., Poot, P., Prior, L., Pyankov, V., Roumet, C., Thomas, S., Tjoelker, M., Veneklaas, E. & Villar, R. (2004) The world-wide leaf economics spectrum. *Nature*, **428**, 821–827.
- Yokozawa, M. & Hara, T. (1995) Foliage profile, size structure and stem diameter plant height relationship in crowded plant-populations. *Annals of Botany*, **76**, 271–285.